SUPPORTING INFORMATION

N-Heterocyclic Phosphenium and Phosphido Nickel Complexes Supported by a Pincer Ligand Framework

Deirdra A. Evers-McGregor, Mark W. Bezpalko, Bruce M. Foxman, Christine M. Thomas*

Department of Chemistry, Brandeis University, 415 South St., Waltham MA, 02453, USA

TABLE OF CONTENTS

Figure S1: ^{1}H NMR spectrum of (PPP)NiCl (**8**) (CD_2Cl_2, 400 MHz)

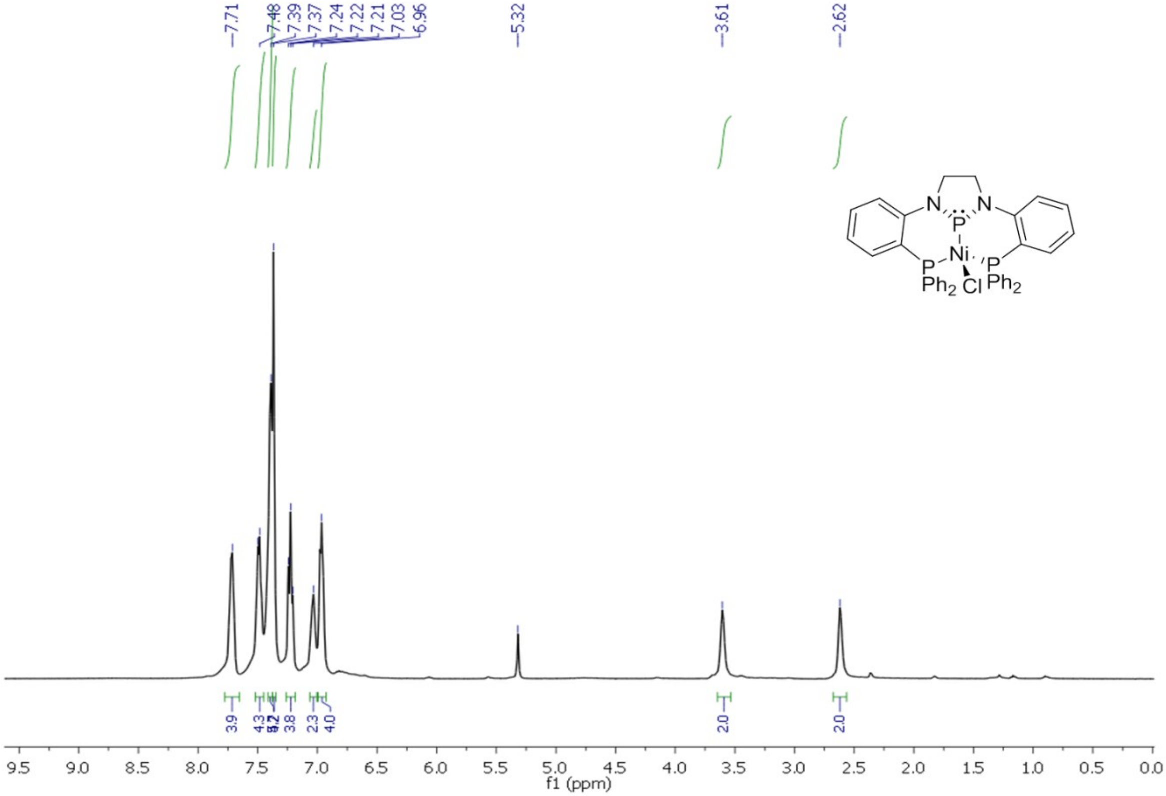

Figure S2: ^{31}P NMR spectrum of (PPP)NiCl (**8**) (CD_2Cl_2, 161.8 MHz)

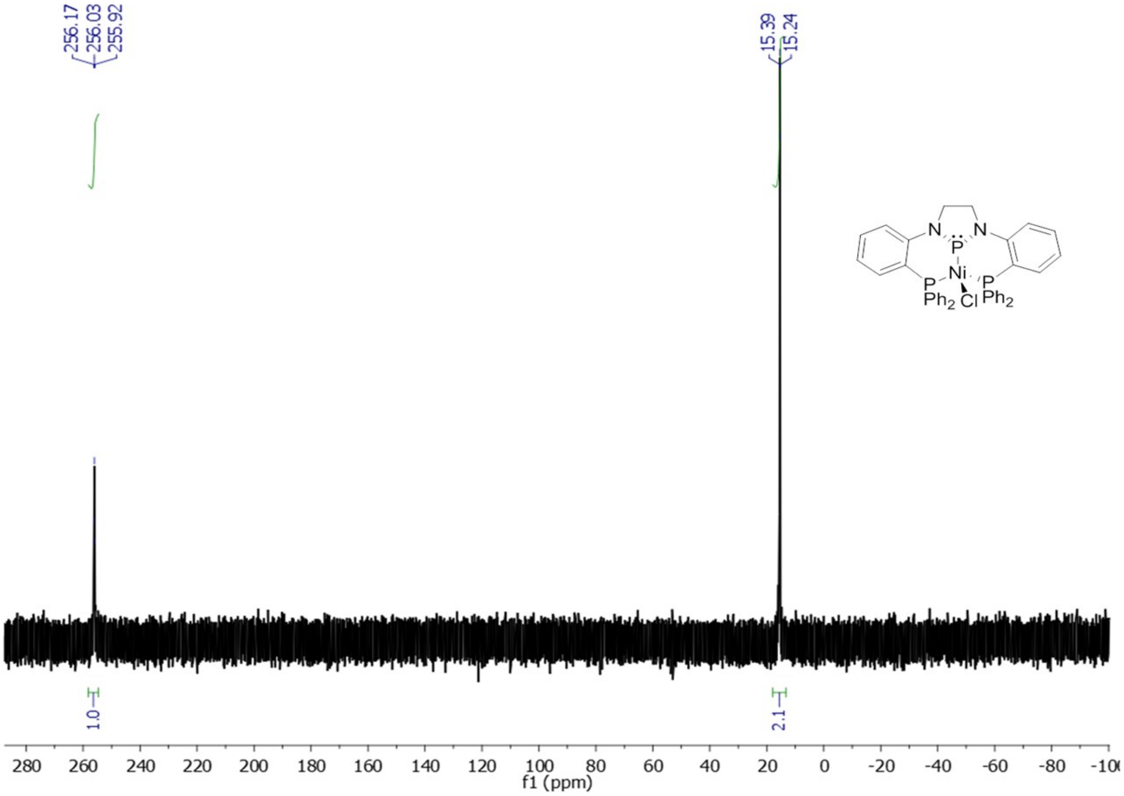

Figure S3: ^{13}C NMR spectrum of (PPP)NiCl (**8**) (CD_2Cl_2, 100.5 MHz)

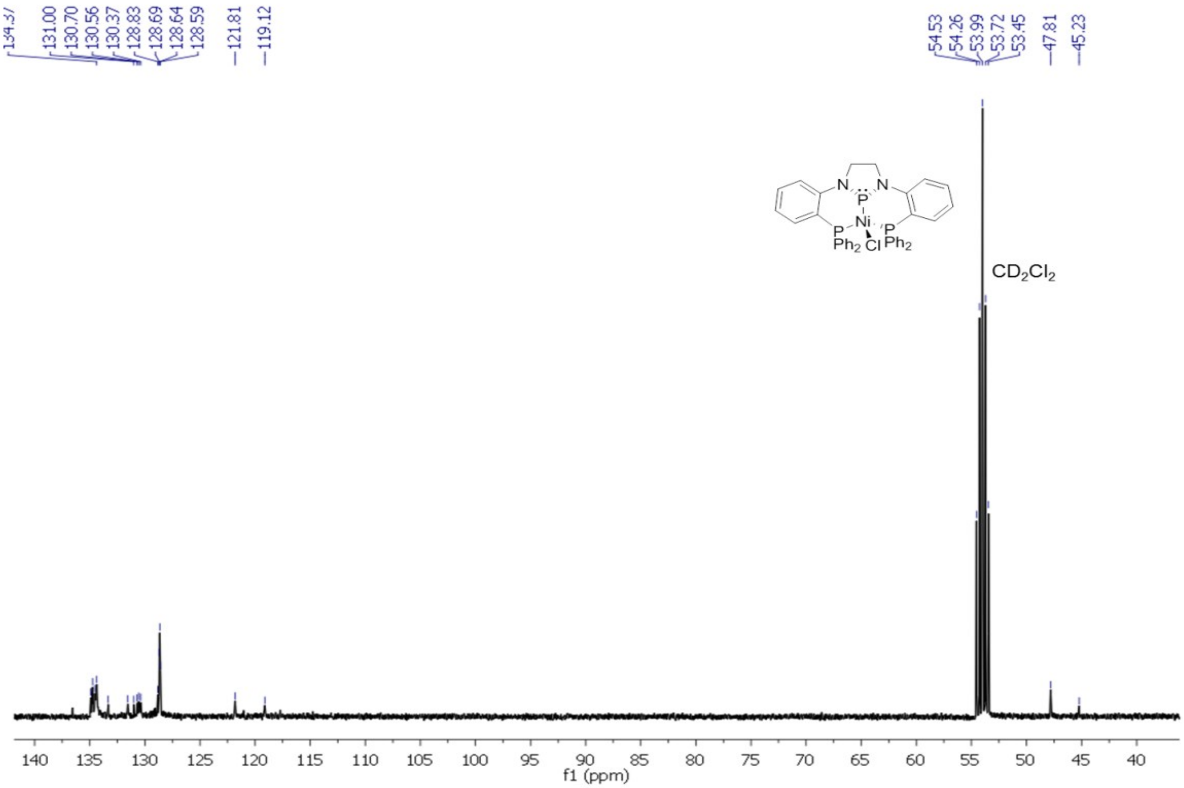

Figure S4: ^{1}H NMR spectrum of $(PPP)_2Ni_3Cl_2$ (**9**) (C_6D_6, 400MHz)

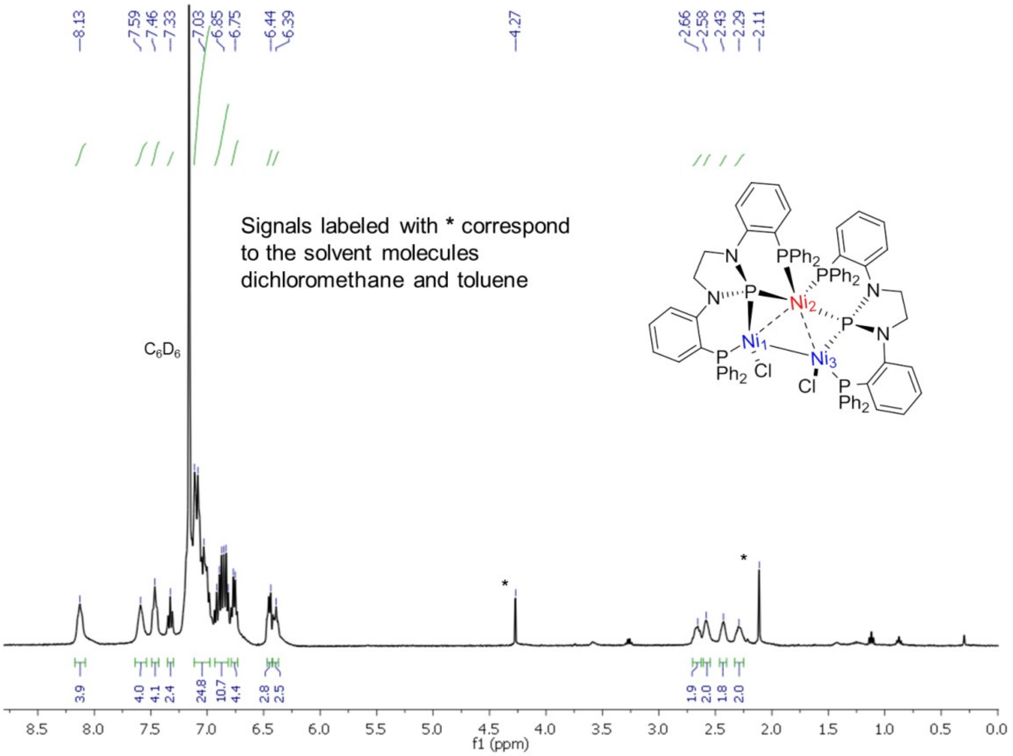

Figure S5: ^{31}P NMR spectrum of $(PPP)_2Ni_3Cl_2$ (**9**) (C_6D_6, 161.8 MHz)

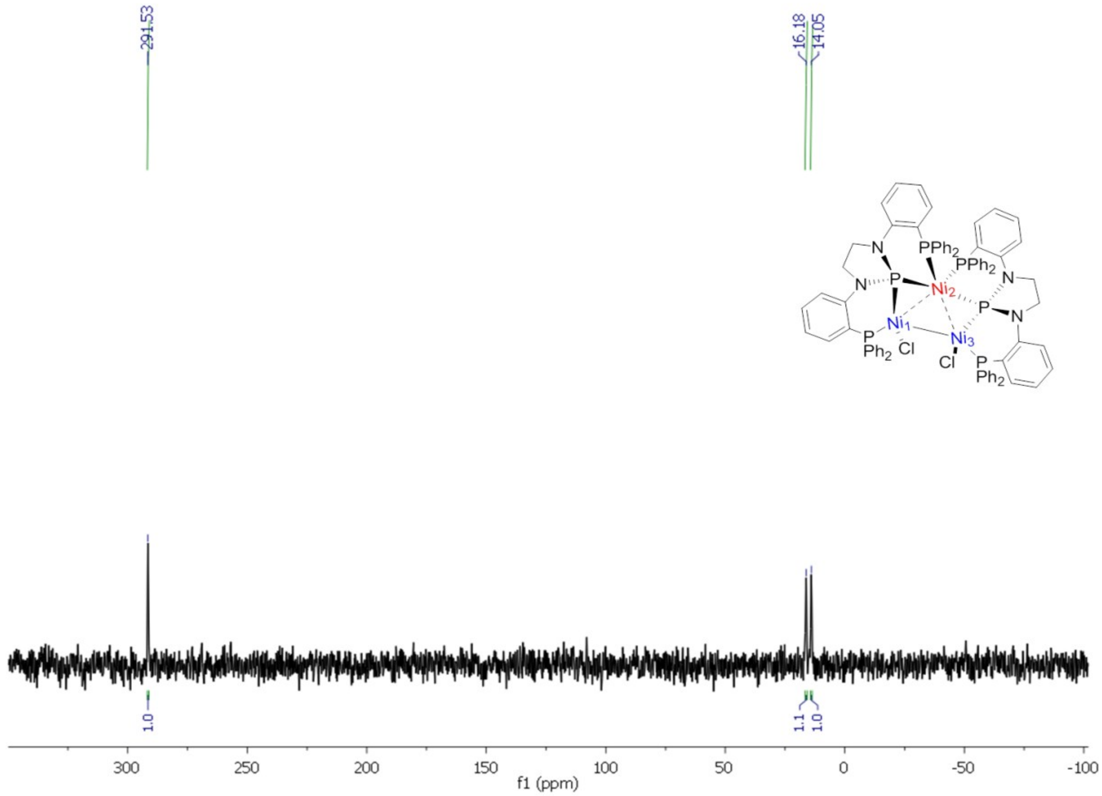

Figure S6: ^{13}C NMR spectrum of $(PPP)_2Ni_3Cl_2$ (**9**) (C_6D_6, 100.5 MHz)

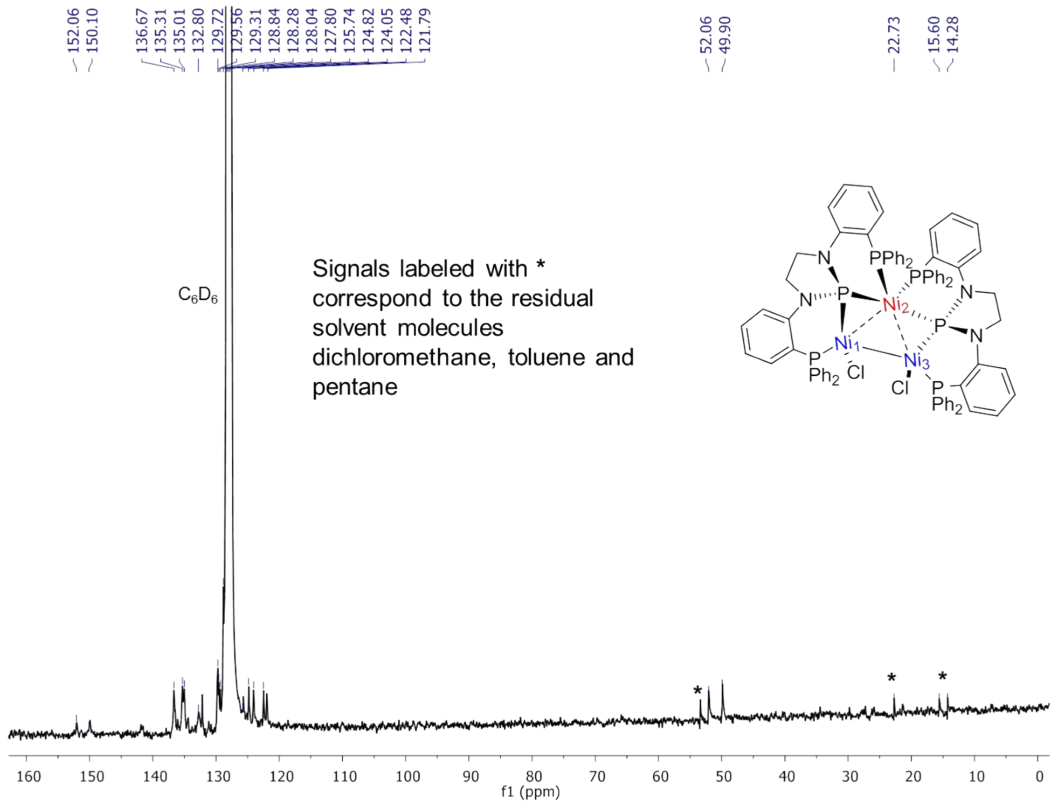

Signals labeled with * correspond to the residual solvent molecules dichloromethane, toluene and pentane

Figure S7: ^{1}H NMR spectrum of [(PPP)Ni]$_2$ (**10**) (C_6D_6, 400 MHz)

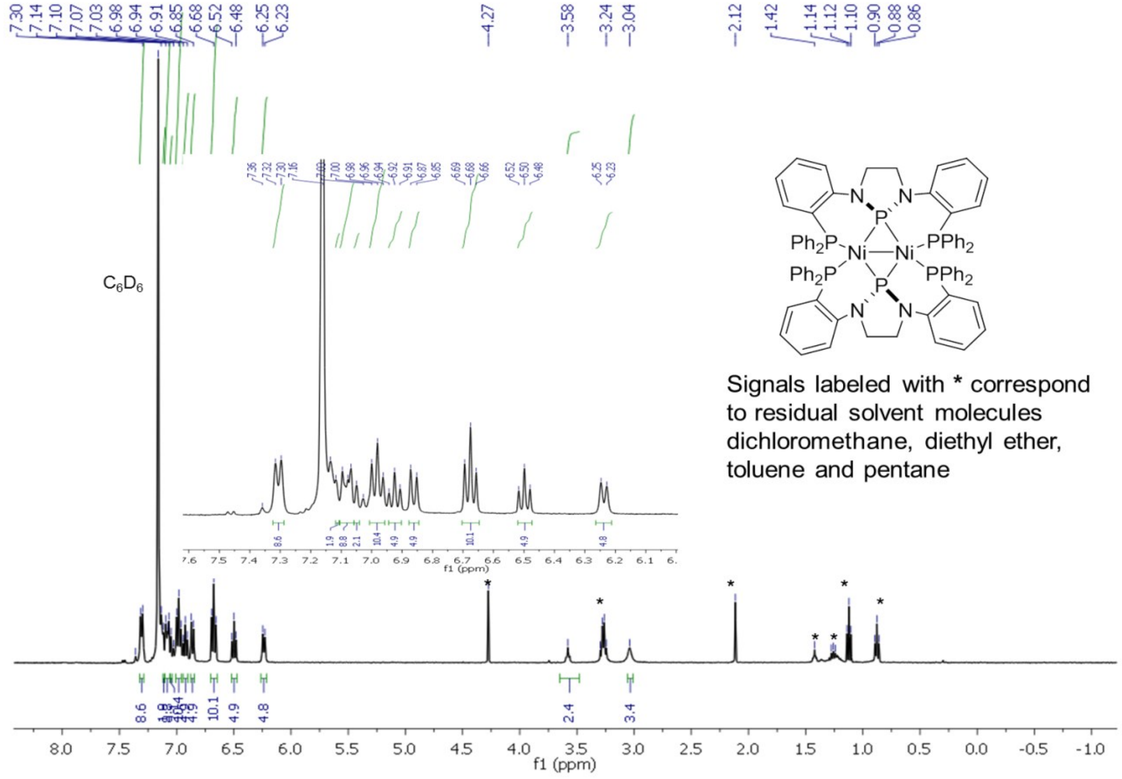

Signals labeled with * correspond to residual solvent molecules dichloromethane, diethyl ether, toluene and pentane

Figure S8: ^{31}P NMR spectrum of [(PPP)Ni]$_2$ (**10**) (C_6D_6, 161.8 MHz)

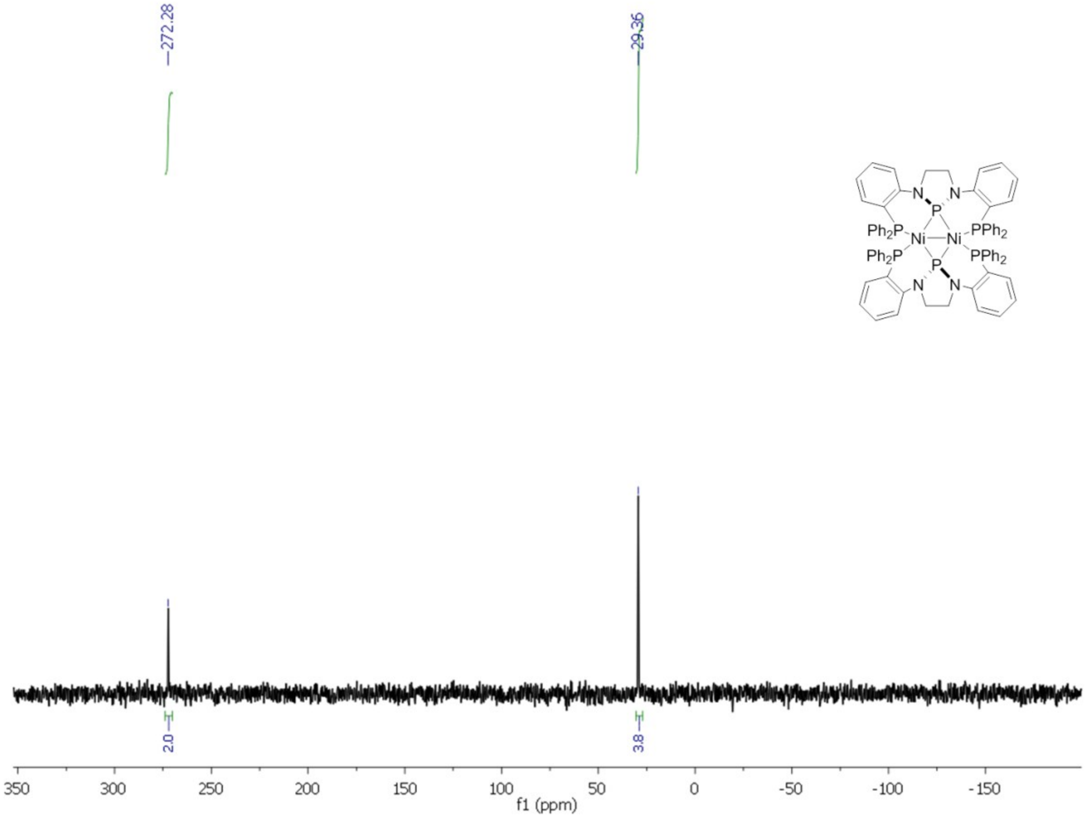

Figure S9: ^{13}C NMR spectrum of $[(PPP)Ni]_2$ (**10**) (C_6D_6, 100.5 MHz)

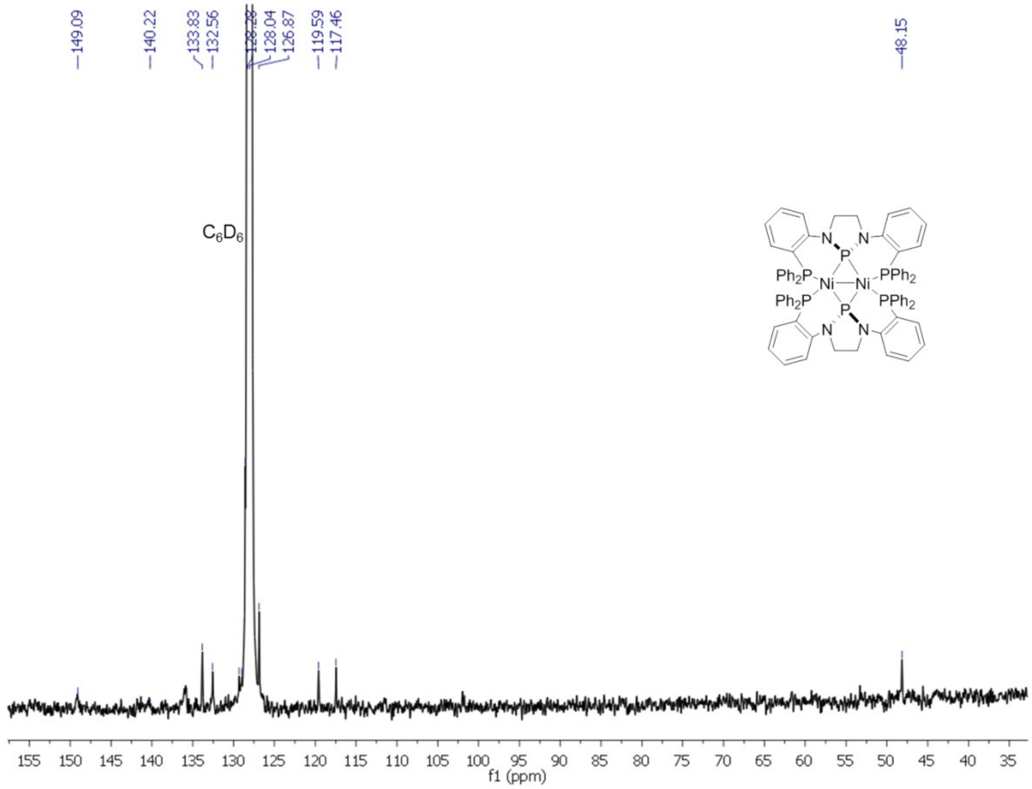

Figure S10: ^{1}H NMR spectrum of $[(PPP)Ni]_2[PF_6]_2$ (**12**) (CD_2Cl_2, 400 MHz)

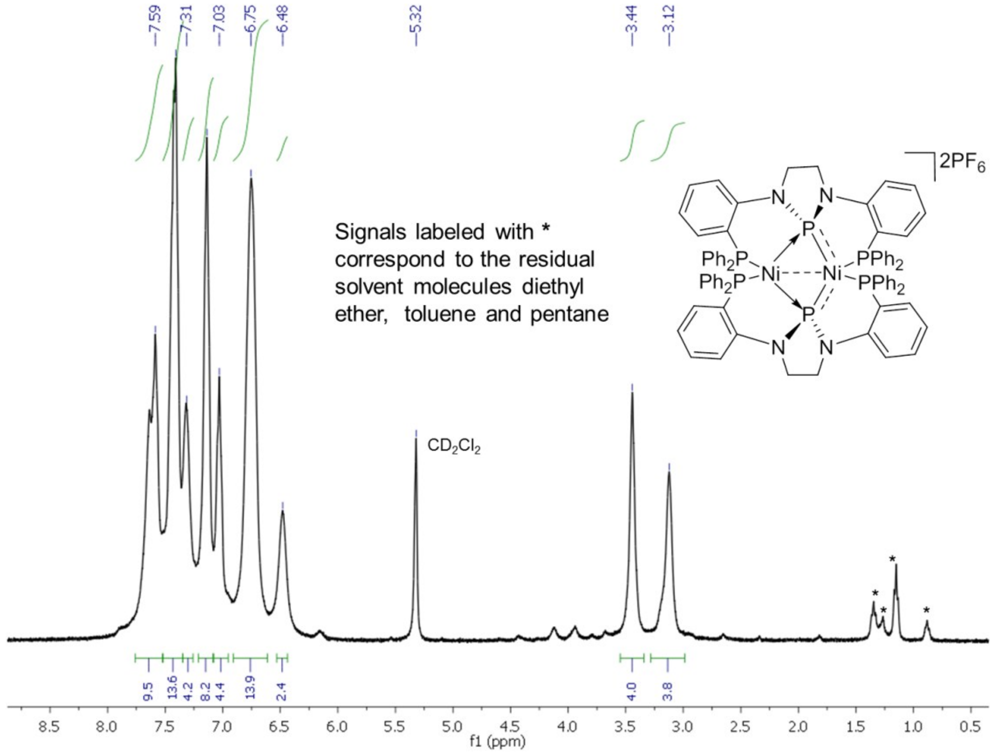

Figure S11: ^{31}P NMR spectrum of $[(PPP)Ni]_2[PF_6]_2$ (**12**) (CD_2Cl_2, 161.8 MHz)

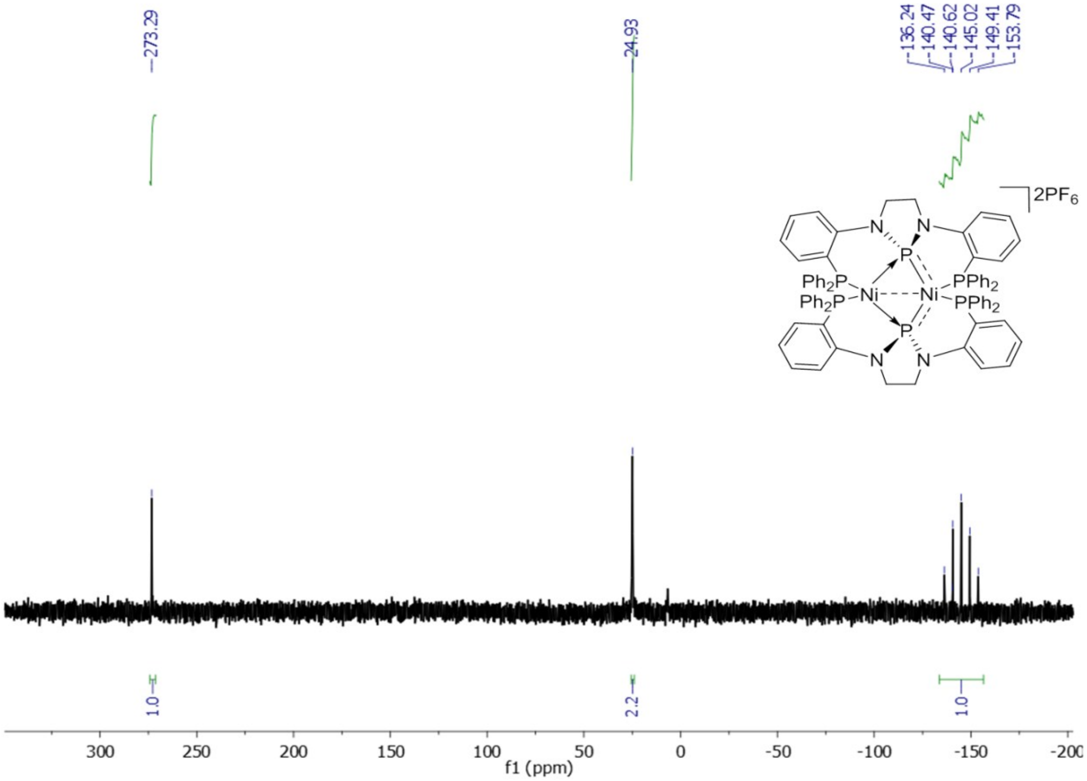

Figure S12: ^{13}C NMR spectrum of $[(PPP)Ni]_2[PF_6]_2$ (**12**) (CD_2Cl_2, 100.5 MHz)

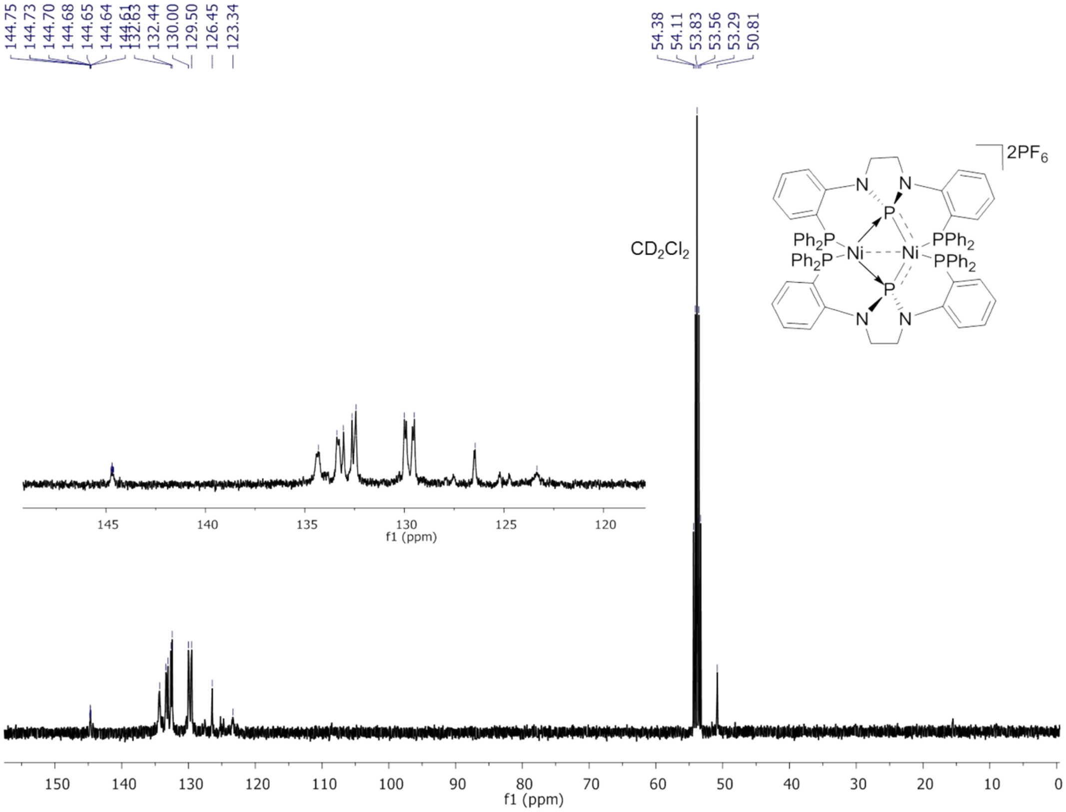

Figure S13: ^{19}F NMR spectrum of $[(PPP)Ni]_2[PF_6]_2$ (**12**) (CD_2Cl_2, 376 MHz)

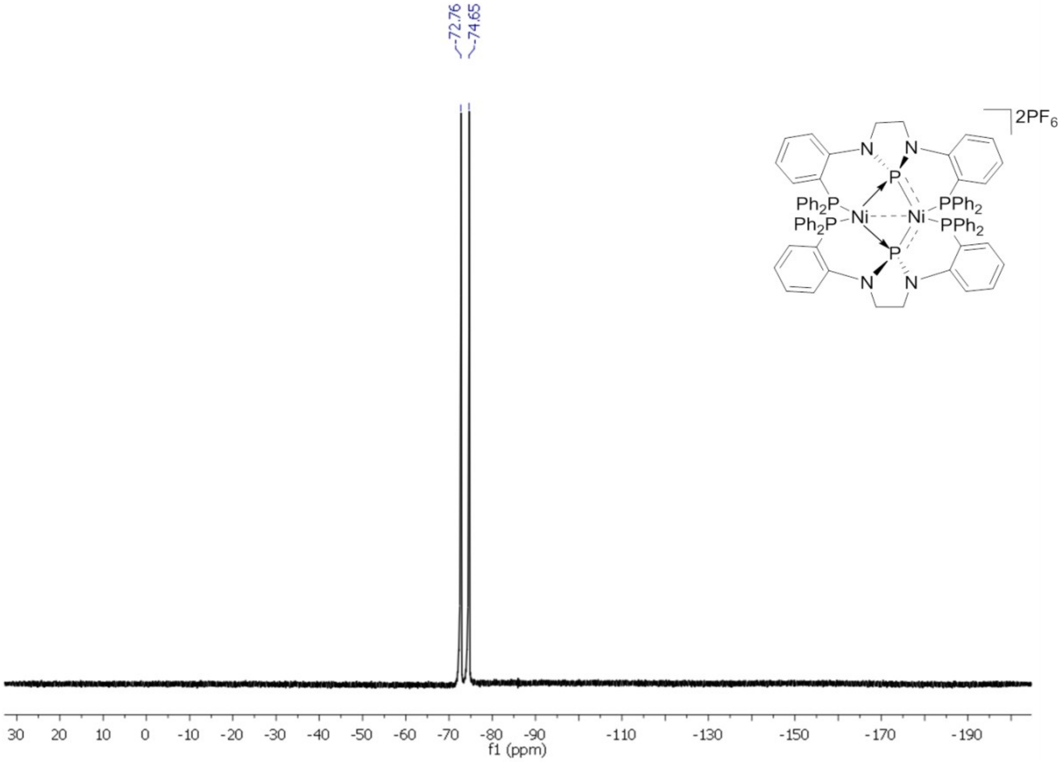

Figure S14: ^{1}H NMR spectrum of $[(PPP)Ni]_2[PF_6]$ (**13**) (CD_2Cl_2, 400 MHz)

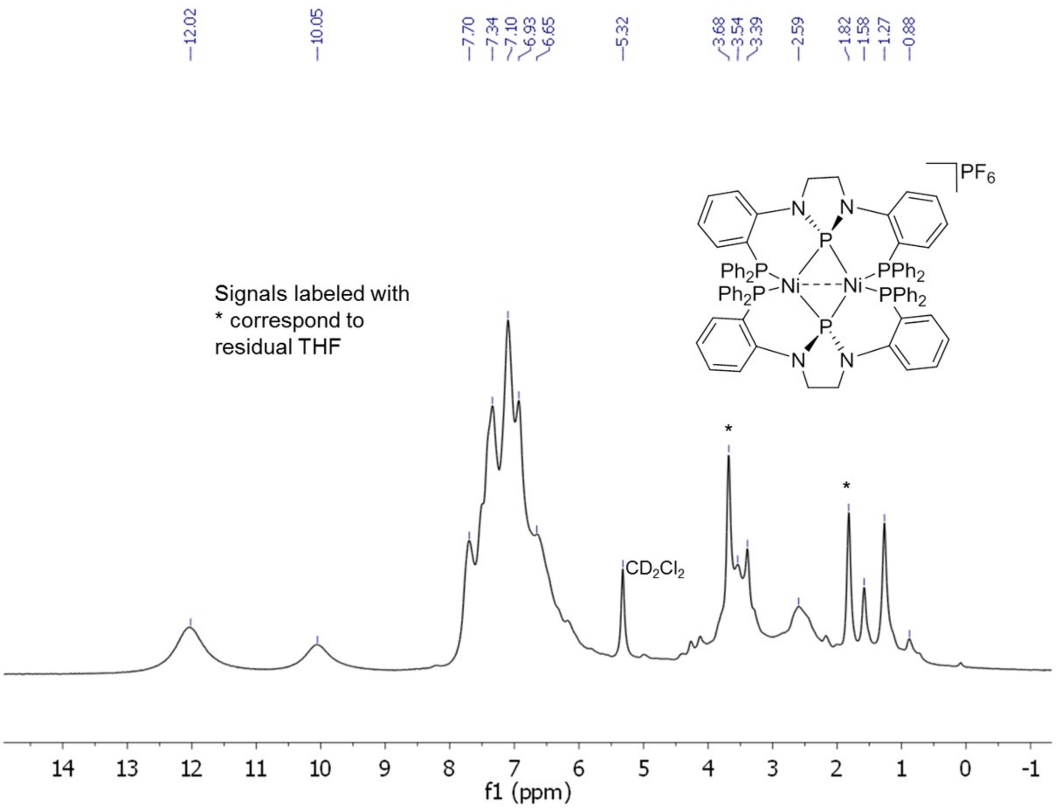
Signals labeled with * correspond to residual THF

Figure S15: Variable Temperature ^{31}P NMR. **A:** ^{31}P NMR (CD_2Cl_2, 161.8 MHz) of $[(PPP)Ni]_2[PF_6]_2$ **(12)** from room temperature to -65°C. **B:** Expansion of the downfield central phosphorus peak. **C:** Expansion of upfield sidearm peaks.

A:

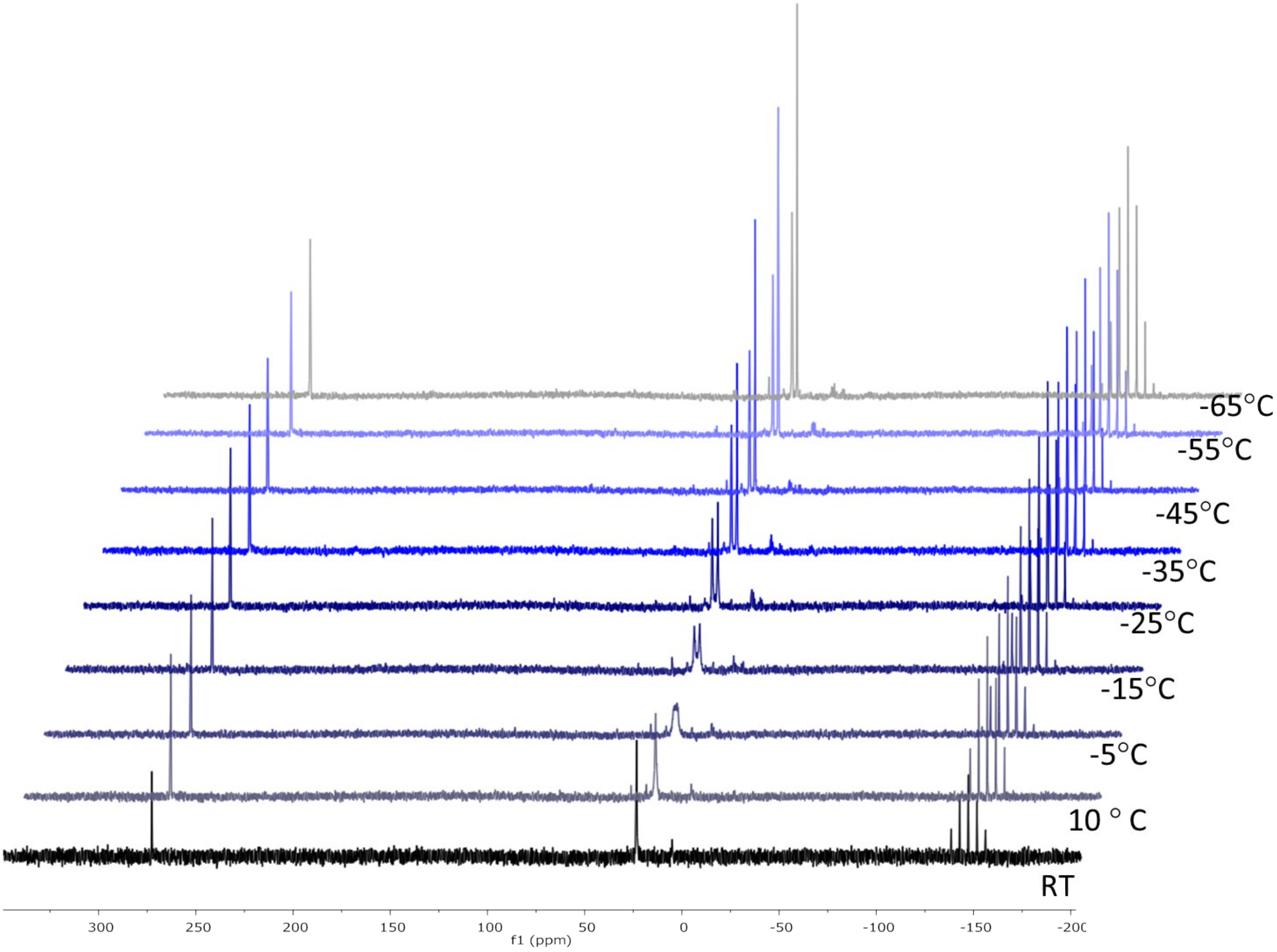

B:

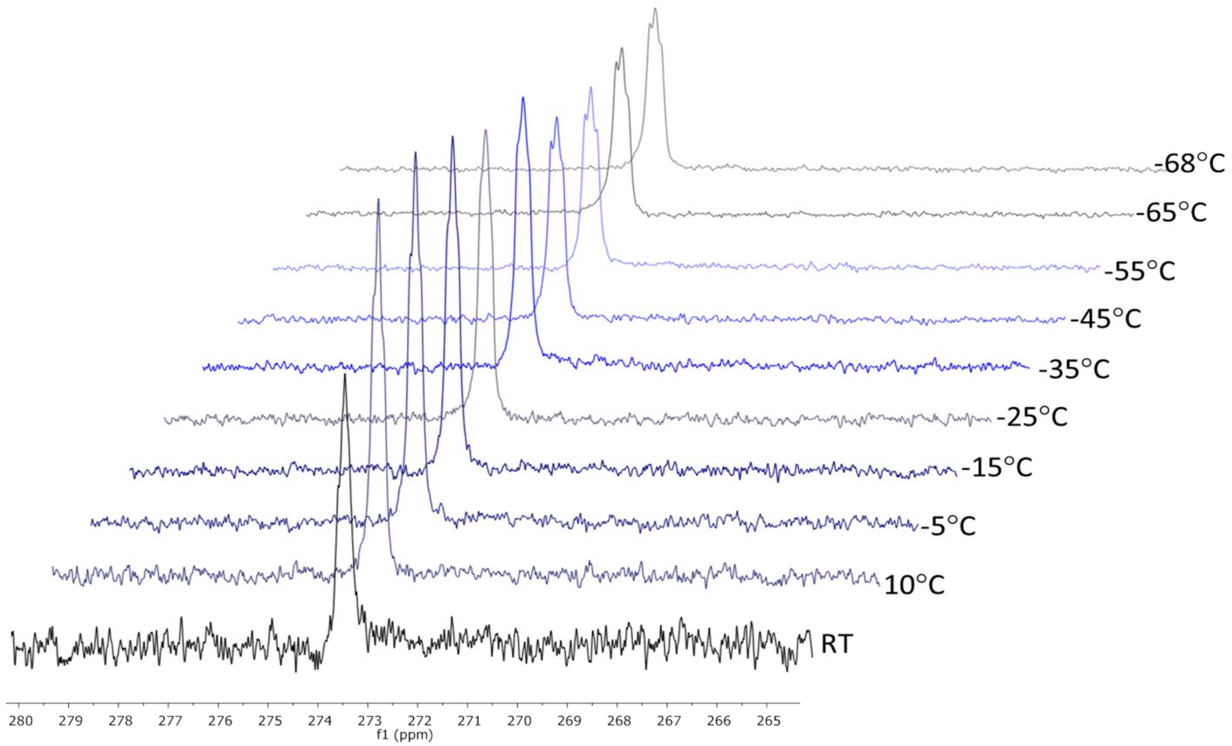
-68°C
-65°C
-55°C
-45°C
-35°C
-25°C
-15°C
-5°C
10°C
RT
280
279
278
277
276
275
274
273
272
271
270
269
268
267
266
265
f1 (ppm)

C:

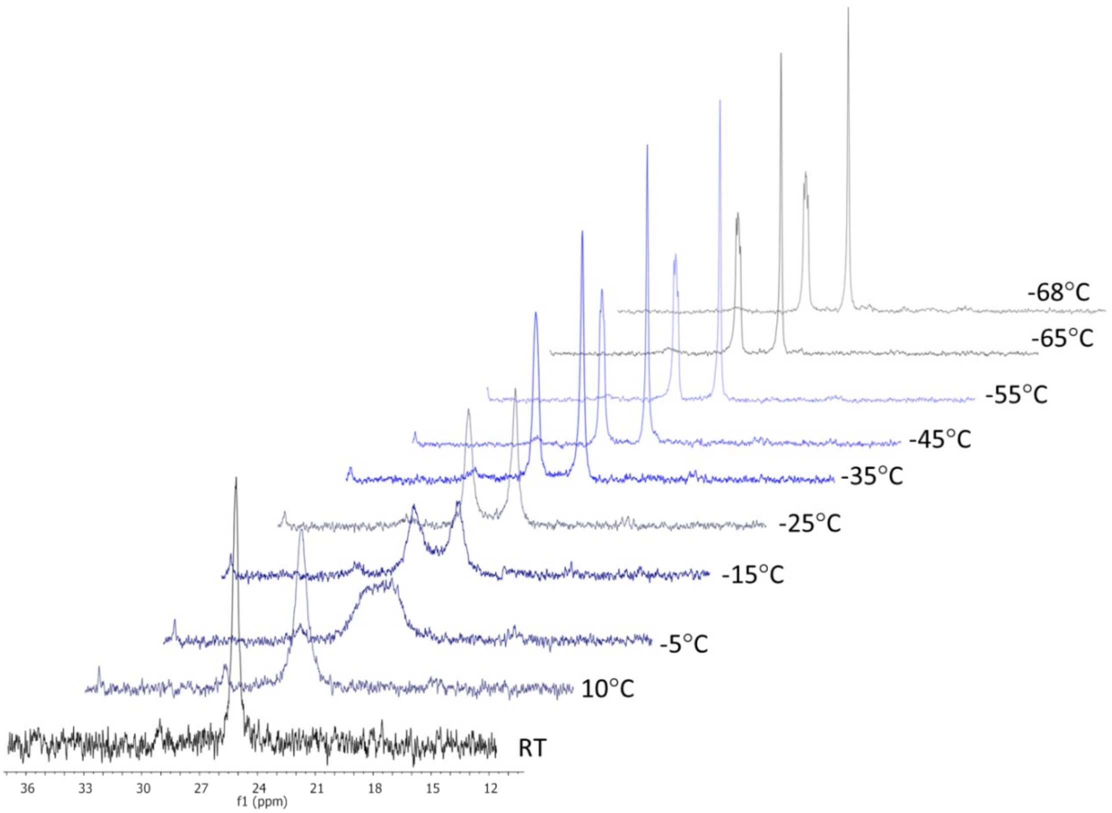
-68°C
-65°C
-55°C
-45°C
-35°C
-25°C
-15°C
-5°C
10°C
RT
36
33
30
27
24
21
18
15
12
f1 (ppm)

Figure S16: Variable temperature ^{1}H NMR (CD_2Cl_2, 400MHz) of $[(PPP)Ni]_2[PF_6]_2$ (**12**) from room temperature to -65°C.

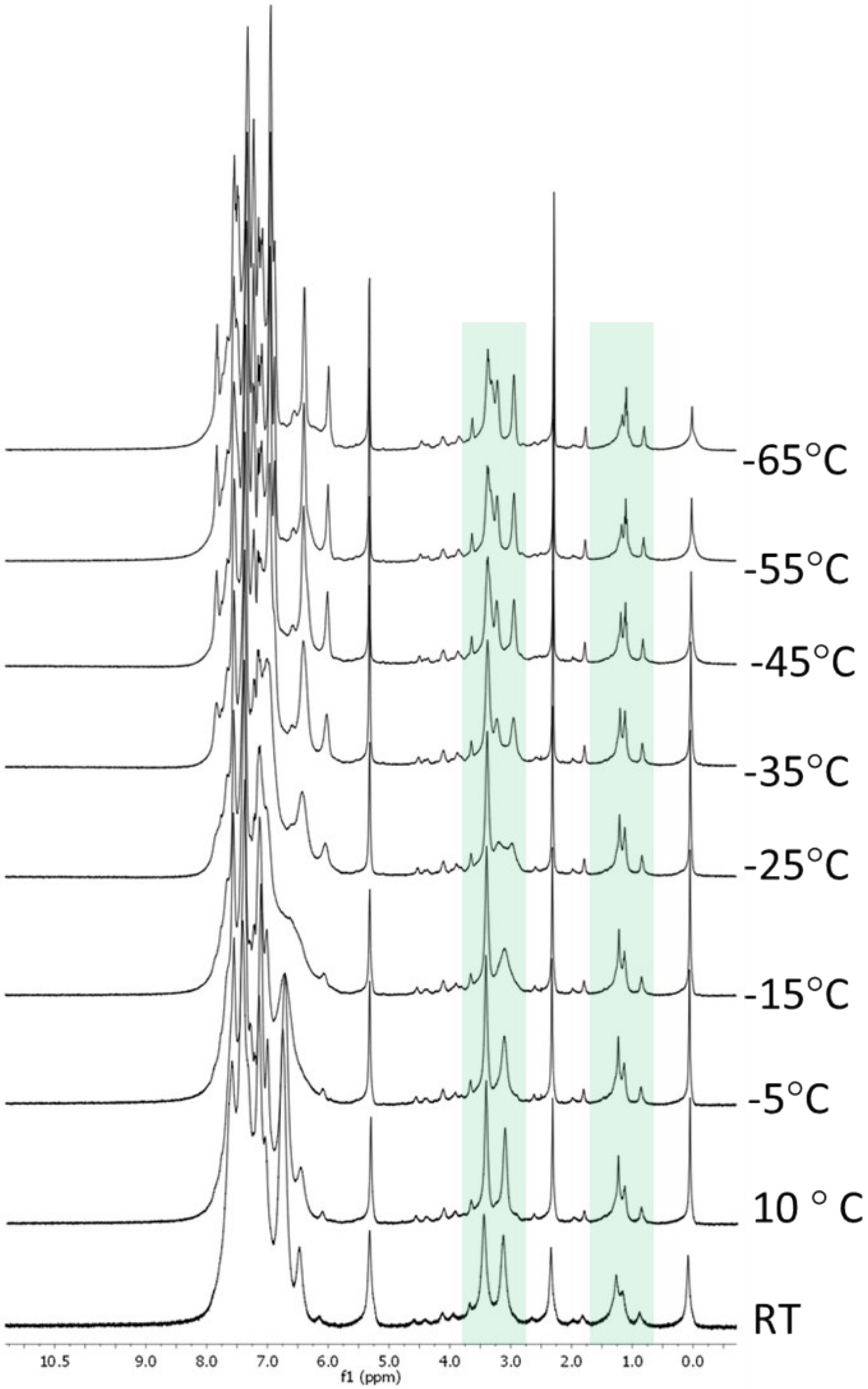

Figure S17: Cyclic Voltammogram of (PPP)NiCl (**8**) (0.4 M [^{t}Bu$_4$N][PF$_6$] in THF, scan rate = 100 mV/s)

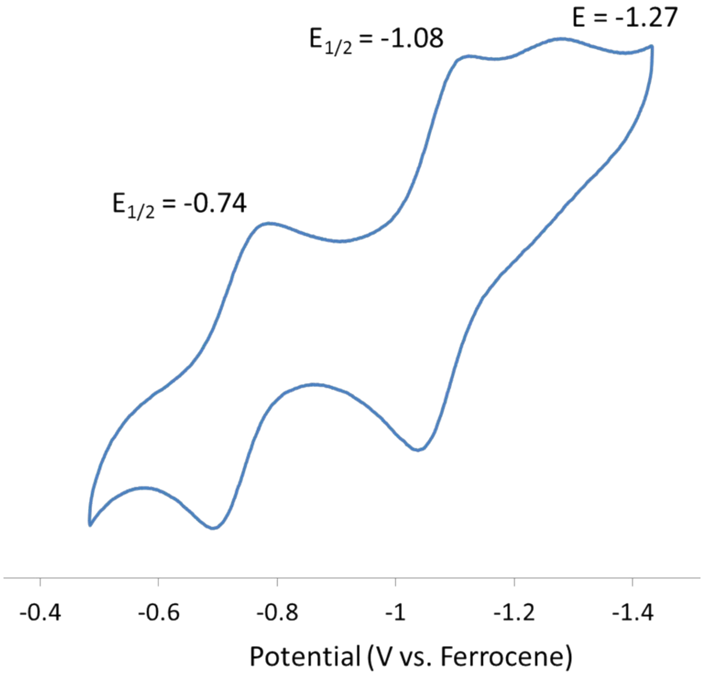

Figure S18: Cyclic Voltammogram of [PPPNi]$_2$ (**10**) (0.4 M [^{t}Bu$_4$N][PF$_6$] in THF, scan rate = 100 mV/s)

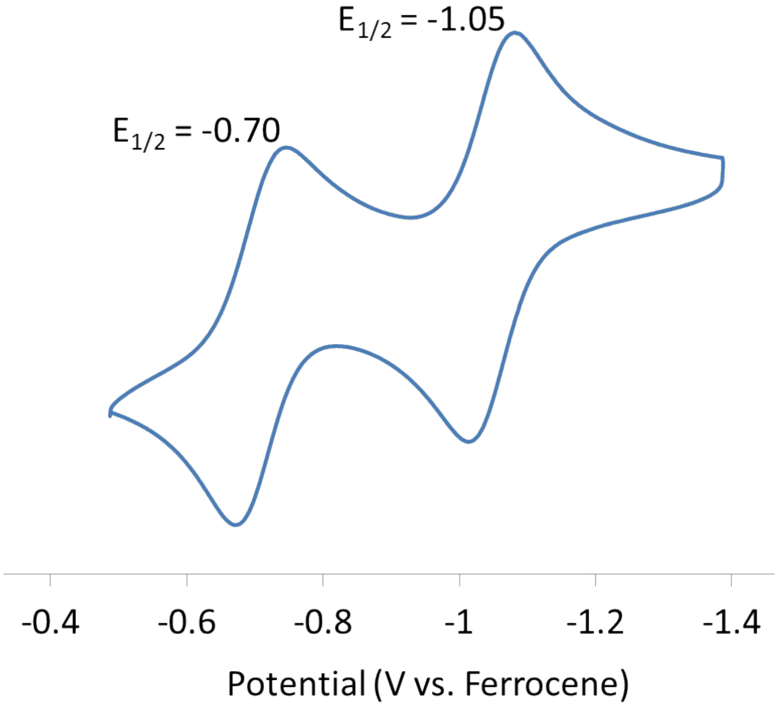

Table S1: Crystallographic Data and Refinement Details for **8, 9, 10** and **12**

	8	**9**	**10**	**12**
chemical formula	$C_{38}H_{32}ClN_2NiP_3$	$C_{86}H_{80}Cl_2N_4Ni_3$	$C_{38}H_{32}N_2P_3Ni_1$	$C_{38}H_{32}F_6N_2Ni_1P_4$
fw	703.77	1618.48	668.32	*813.28*
T (K)	120	120	120	120
λ (Å)	0.71073	0.71073	0.71073	0.71073
a (Å)	9.9478(3)	31.6465(7)	16.6009(8)	26.0844(7)
b (Å)	12.3725(4)	31.6465(7)	16.6009(8)	13.0789(4)
c (Å)	28.7138(9)	30.383830(8)	25.9072(16)	23.9074(7)
α (°)	87.7587(16)	90	90	90
β (°)	82.8945(17)	90	90	121.5730(11)
γ (°)	71.3079(16)	90	90	90
V (Å^3)	3321.95	30428.6	7139.8(4)	6948.8(2)
space group	$P\bar{1}$	$I4_1/a$	$I\bar{4}c2$	$C2/c$
Z, Z'	4, 2	16, 1	8, ½	8, 1
D_{calc} (g/cm^3)	1.407	1.413	1.243	1.555
μ (cm^{-1})	8.40	9.82	7.05	8.08
R1 $(I > 2\sigma(I))$, wR2^a	0.0372, 0.0993	0.0409, 0.0959	0.0514, 0.1284	0.0420, 0.1228

$R1 = \Sigma||F_o| - |F_c||/\Sigma|F_o|$, $wR2 = \{\Sigma[w(F_o^2 - F_c^2)^2]/\Sigma[w(F_o^2)^2]\}^{1/2}$

Figure S19: Fully-labeled ellipsoid representation of **8**

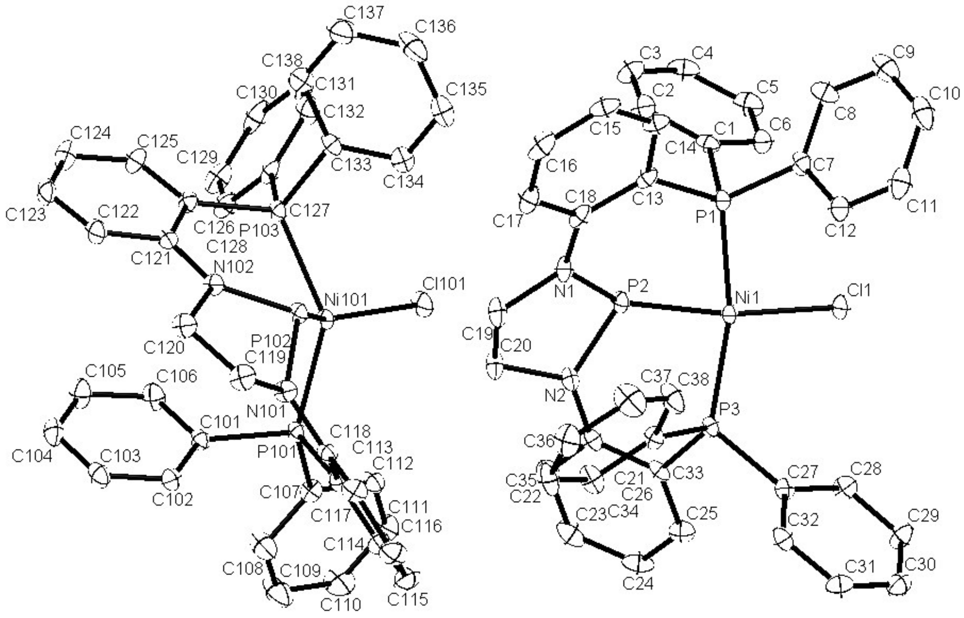

X-Ray data collection, solution, and refinement for 8. All operations were performed on a Bruker-Nonius Kappa Apex2 diffractometer, using graphite-monochromated MoKα radiation. All diffractometer manipulations, including data collection, integration, scaling, and absorption corrections were carried out using the Bruker Apex2 software.[1] Preliminary cell constants were obtained from three sets of 12 frames. Data collection was carried out at 120K, using a frame time of 20 sec and a detector distance of 60 mm. The optimized strategy used for data collection consisted of six phi and four omega scan sets, with 0.5° steps in phi or omega; completeness was 99.7%. A total of 3629 frames were collected. Final cell constants were obtained from the xyz centroids of 9920 reflections after integration.

From the systematic absences, the observed metric constants and intensity statistics, space group $P\bar{1}$ was chosen initially; subsequent solution and refinement confirmed the correctness of this choice. The structure was solved using SIR-92,[2] and refined (full-matrix-least squares) using the

Oxford University Crystals for Windows program.[3] The asymmetric unit contains two molecules of the complex, and likely one-half molecule of DCM, modeled using the SQUEEZE procedure (see below) (for the complex, Z = 4; Z' = 2). The second molecule is numbered similarly to the first, with atom sequence numbers exactly 100 greater than those of the reference molecule. All non-hydrogen atoms were refined using anisotropic displacement parameters. After location of H atoms on electron-density difference maps, the H atoms were initially refined with soft restraints on the bond lengths and angles to regularize their geometry (C---H in the range 0.93--0.98 Å and Uiso (H) in the range 1.2-1.5 times Ueq of the parent atom), after which the positions were refined with riding constraints.[4] During the structure solution, electron density difference maps revealed that there was considerable disordered associated with a DCM solvent molecule, which could not be successfully modeled. From history, the remaining solvate was likely DCM in a volume of 155.7 Å3 per unit cell (4.7%). It appeared that the cavity area contained about one DCM molecule, located near an inversion center at (0, 0, ½), as shown in the bc projection below.[5]

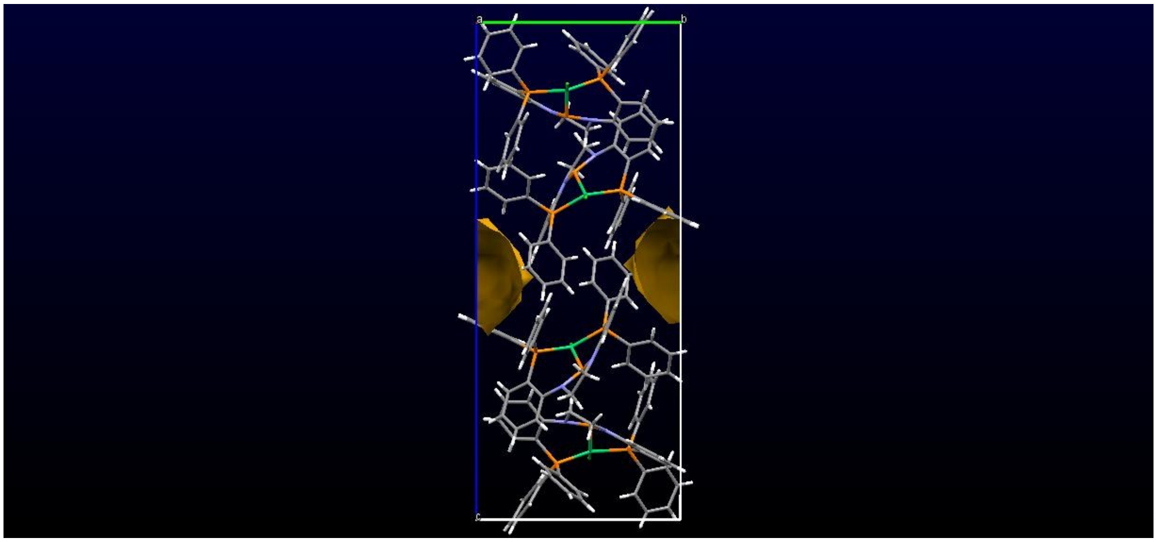

Modeling with or without restraints was unsuccessful, as was step by step acquisition of peaks using successive electron density difference maps. Thus, the structure factors were modified using the PLATON SQUEEZE[6,7] technique, in order to produce a "solvate-free" structure factor set.

PLATON reported a total electron density of 34 e^- per unit cell, likely representing one DCM molecule, consistent with our earlier observations. Use of the SQUEEZE technique resulted in a decrease of ca. 2.7 % in R. The final least-squares refinement converged to R1 = 0.0372 ($I > 2\sigma(I)$, 12260 data) and wR2 = 0.0993 (F2, 16068 data, 811 parameters). The final CIF is available as supporting material.

Figure S20: Fully-labeled ellipsoid representation of **9**

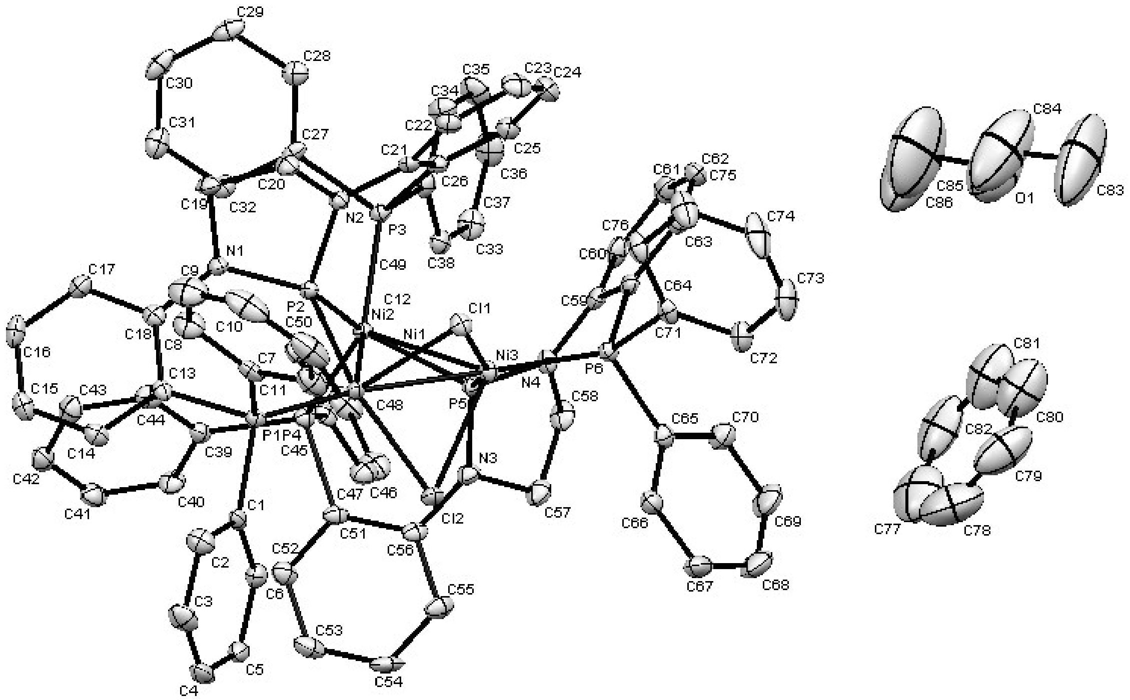

X-Ray data collection, solution, and refinement for 9. All operations were performed on a Bruker-Nonius Kappa Apex2 diffractometer, using graphite-monochromated MoKα radiation. All diffractometer manipulations, including data collection, integration, scaling, and absorption corrections were carried out using the Bruker Apex2 software.[1] Preliminary cell constants were obtained from three sets of 12 frames. Data collection was carried out at 120K, using a frame time of 40 sec and a detector distance of 60 mm. The optimized strategy used for data collection consisted of one phi and three omega scan sets, with 0.5° steps in phi or omega; completeness was 99.9 %. A total of 994 frames were collected. Final cell constants were obtained from the xyz centroids of 9966 reflections after integration.

From the systematic absences, the observed metric constants and intensity statistics, space group $I4_1/a$ was chosen initially; subsequent solution and refinement confirmed the correctness of this choice. The structure was solved using *SuperFlip*,[8] and refined (full-matrix-least squares) using the Oxford University *Crystals for Windows* program.[3,4] The asymmetric unit contains one molecule of the complex, and one benzene solvate, one ether solvate and likely a quarter molecule of ether, modeled using the SQUEEZE procedure (see below) (for the complex $Z = 16$; $Z' = 1$). All non-hydrogen atoms were refined using anisotropic displacement parameters. After location of H atoms on electron-density difference maps, the H atoms were initially refined with soft restraints on the bond lengths and angles to regularize their geometry (C---H in the range 0.93--0.98 Å and U_{iso} (H) in the range 1.2-1.5 times U_{eq} of the parent atom), after which the positions were refined with riding constraints.[4] During the structure solution, electron density difference maps revealed that there were considerable disordered solvent molecules which could not be successfully modeled. From history, the remaining solvate was likely ether in a volume of 749.2 Å^3 per unit cell (2.5%). It appeared that the cavity area contained about four ether molecules, located near the $\bar{4}$ positions at (0, ¼, 1/8), (0, ¾, 7/8), (½, ¼, 3/8), and (½, ¾, 5/8) as shown in the *ab* projection below.[5]

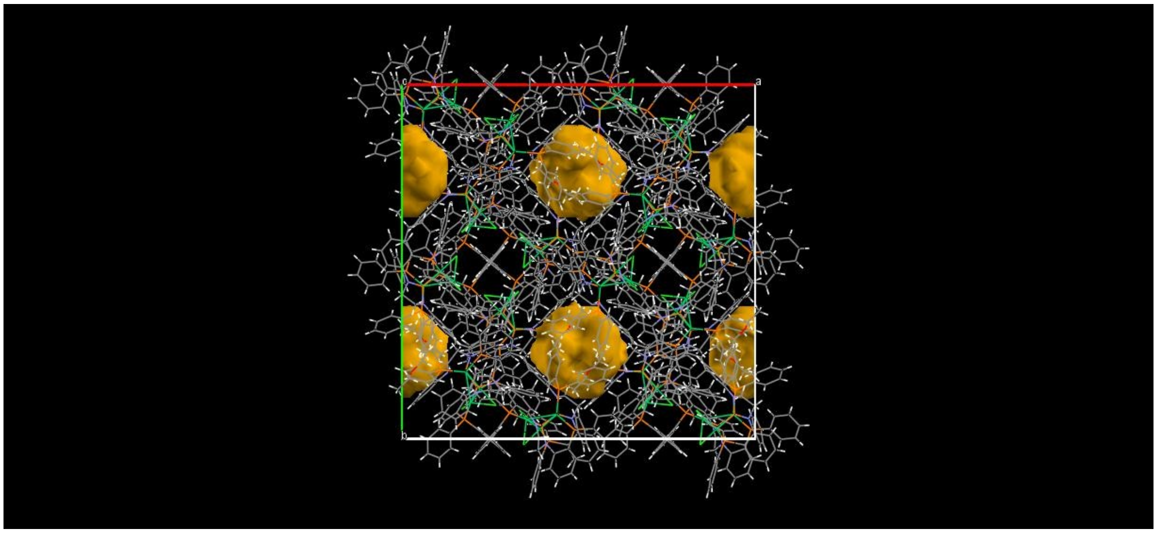

Modeling with or without restraints was unsuccessful, as was step by step acquisition of peaks using successive electron density difference maps. Thus, the structure factors were modified using the PLATON SQUEEZE[6,7] technique, in order to produce a "solvate-free" structure factor set. PLATON reported a total electron density of 165 e$^-$ per unit cell, likely representing four ether molecules, consistent with our earlier observations. Use of the SQUEEZE technique resulted in a decrease of *ca.* 0.4 % in *R*. Distance restraint was used for C atoms (85) to (86) located on the ether molecule. The final least-squares refinement converged to $R_1 = 0.0409$ ($I > 2\sigma(I)$, 10952 data) and $wR_2 = 0.0959$ (F^2, 15039 data, 919 parameters). The final CIF is available as supporting material.

Figure S21: Fully-labeled ellipsoid representation of **10**

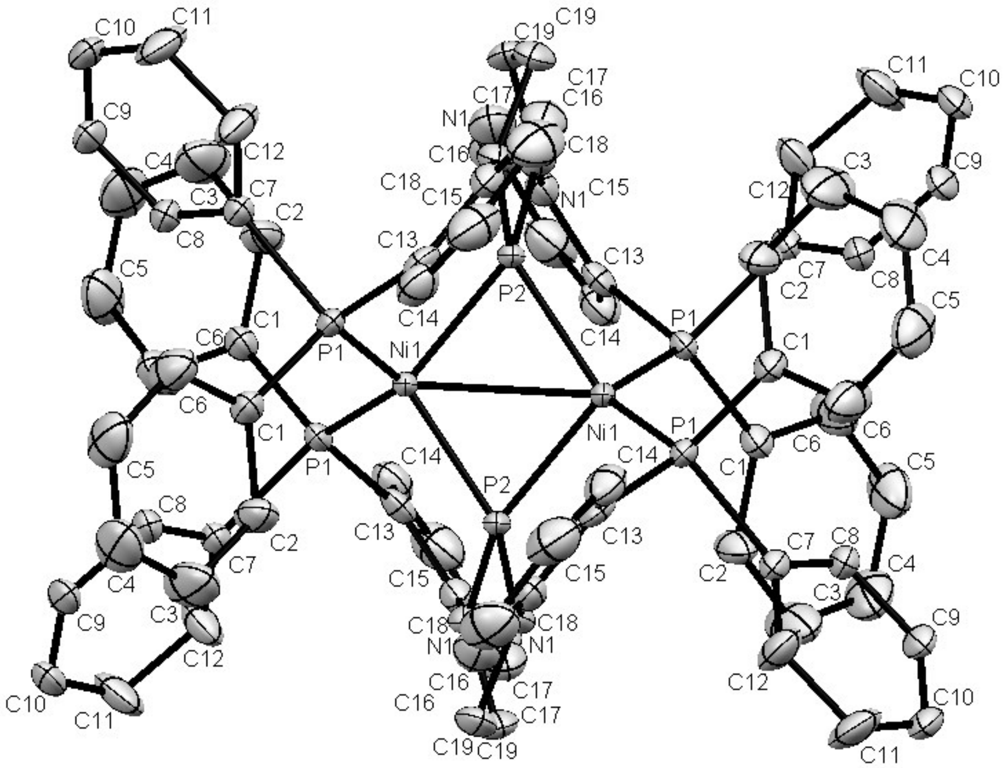

X-Ray data collection, solution, and refinement for 10. All operations were performed on a Bruker-Nonius Kappa Apex2 diffractometer, using graphite-monochromated MoKα radiation. All diffractometer manipulations, including data collection, integration, scaling, and absorption corrections were carried out using the Bruker Apex2 software.[1] Preliminary cell constants were obtained from three sets of 12 frames. Data collection was carried out at 120K, using a frame time of 20 sec and a detector distance of 60 mm. The optimized strategy used for data collection consisted of five phi and three omega scan sets, with 0.5° steps in phi or omega; completeness was 99.1 %. A total of 3626 frames were collected. Final cell constants were obtained from the xyz centroids of 9755 reflections after integration.

From the systematic absences, the observed metric constants and intensity statistics, space group $I\bar{4}c2$ was chosen initially; subsequent solution and refinement confirmed the correctness of this choice. The structure was solved using *SIR-92*,[2] and refined (full-matrix-least squares) using the Oxford University *Crystals for Windows* program.[3] The asymmetric unit contains one half-molecule of the complex, and likely one half-molecule of pentane, modeled using the SQUEEZE procedure (see below) (for the complex, $Z = 8$; $Z' = ½$). All non-hydrogen atoms were refined using anisotropic displacement parameters. After location of H atoms on electron-density difference maps, the H atoms were initially refined with soft restraints on the bond lengths and angles to regularize their geometry (C---H in the range 0.93--0.98 Å and U_{iso} (H) in the range 1.2-1.5 times U_{eq} of the parent atom), after which the positions were refined with riding constraints.[4] During the structure solution, electron density difference maps revealed that there were considerable disordered solvent molecules which could not be successfully modeled. From history, the remaining solvate was likely pentane in a volume of 1234.5 Å^3 per unit cell (17.3%). It appeared that the cavity area contained about eight pentane molecules, located in pairs near the four 222 positions at (0, ½, 0); (0, ½, ½); (½, 0, ½); (½, 1, 0) as shown in the *bc* projection below.[5]

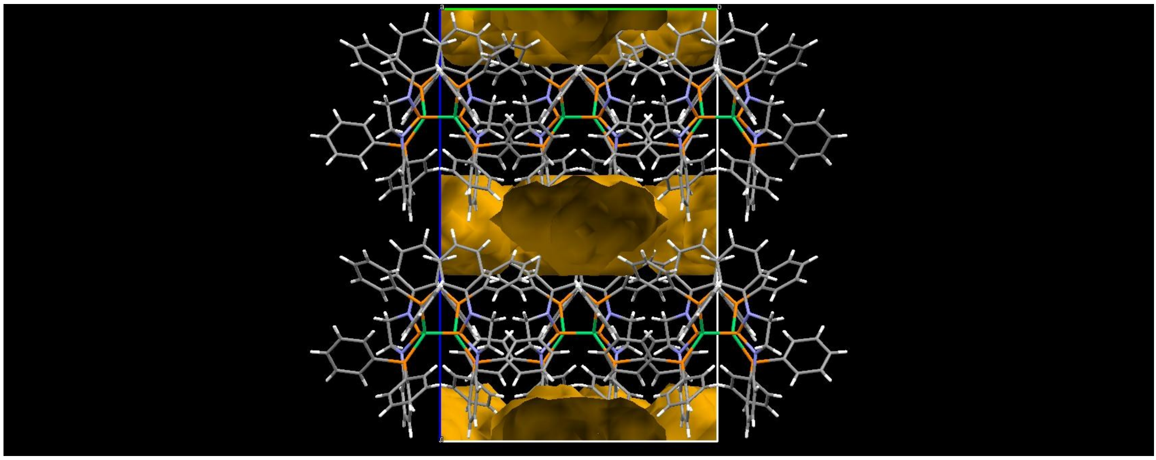

Modeling with or without restraints was unsuccessful, as was step by step acquisition of peaks using successive electron density difference maps. Thus, the structure factors were modified using the PLATON SQUEEZE[6] technique, in order to produce a "solvate-free" structure factor set. PLATON reported a total electron density of 350 e$^-$ per unit cell, likely representing eight pentane molecules, consistent with our earlier observations. Use of the SQUEEZE technique resulted in a decrease of *ca.* 3.8 % in *R*. The absolute structure was established by using Flack parameter refinement (x = 0.010(15)). The final least-squares refinement converged to $R_1 = 0.0514$ ($I > 2\sigma(I)$, 4015 data) and $wR_2 = 0.1284$ (F^2, 4786 data, 200 parameters). The final CIF is available as supporting material.

Figure S22: Fully-labeled ellipsoid representation of **12**

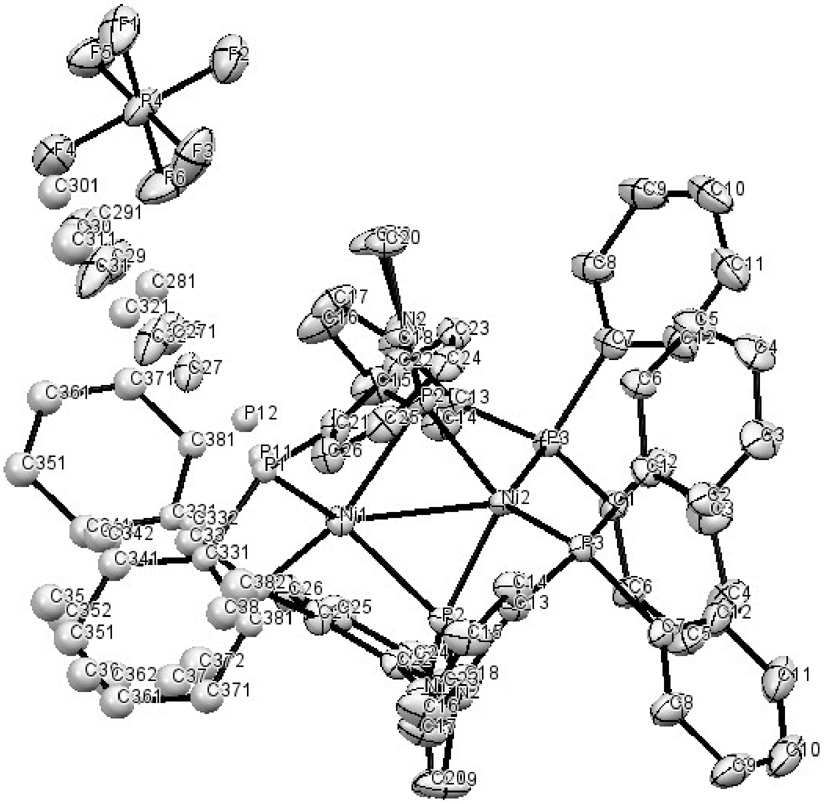

X-Ray data collection, solution, and refinement for 12. All operations were performed on a Bruker-Nonius Kappa Apex2 diffractometer, using graphite-monochromated MoKα radiation. All diffractometer manipulations, including data collection, integration, scaling, and absorption corrections were carried out using the Bruker Apex2 software.[1] Preliminary cell constants were obtained from three sets of 12 frames. Data collection was carried out at 120K, using a frame time of 20 sec and a detector distance of 60 mm. The optimized strategy used for data collection consisted of four phi and four omega scan sets, with 0.5° steps in phi or omega; completeness was 99.6 %. A total of 1814 frames were collected. Final cell constants were obtained from the xyz centroids of 9906 reflections after integration.

From the systematic absences, the observed metric constants and intensity statistics, space group *C*2/*c* was chosen initially; subsequent solution and refinement confirmed the correctness of this choice. The structure was solved using *SIR-92*,[2] and refined (full-matrix-least squares) using the Oxford University *Crystals for Windows* program.[3] The asymmetric unit contains one molecule of the complex ($Z = 8$; $Z' = 1$). All ordered non-hydrogen atoms were refined using anisotropic displacement parameters. After location of H atoms on electron-density difference maps, the H atoms were initially refined with soft restraints on the bond lengths and angles to regularize their geometry (C---H in the range 0.93--0.98 Å and U_{iso} (H) in the range 1.2-1.5 times U_{eq} of the parent atom), after which the positions were refined with riding constraints.[4] At a later stage in the refinement it became apparent that disorder was present in the vicinity of ligand atom P(1). The disorder, which could be modeled only partially, involves positional disorder of atom P(1), but in an unusual way. There are three components to the disorder; the sum of the occupancies of the three components was constrained to sum to 1.0. Components 1 and 2 involve minor positional disorder of the ligand P atom, with P(1) at a refined occupancy of 0.474(9) [Ni(1)-P(1), 2.218(2) Å] and P(11) at 0.463(9) [Ni(1)-P(11), 2.273(2) Å]; the difference between the two Ni-P bond lengths is unlikely to be experimentally significant owing to the disorder and the proximity (0.22 Å) of atoms P(1) and P(11). The remaining ligand atom P(12), component 3, occupancy 0.063(2), is in an "arm-off" position, more distant from the other component P atoms (0.85 and 0.66 Å from P(1) and P(11), respectively, with a Ni(1)-P(12) distance of 2.808(10) Å. The P(1)//P(11)//P(12) disordered set is in (a) an appropriate position such that disorder is minimal and not resolvable for phenyl ring C(21)-C(26); (b) the set is in an position which allows all three phenyl rings to be resolved for ring sets C(33)-C(36)/C(331)-C(361)/C(332)-C(362), and, finally (c) in a position such that the disorder could only partially be resolved for the last set, C(27)-C(32)/C(271)-C(321). For the last set, the C(27)-C(32) atoms comprise the component 1 and component 2 sets (not resolvable in this case) with occupancy of 0.474 + 0.463 = 0.937(9), while the second set, occupancy 0.063(2), C(271)-C(321), arises from the component 3 disorder. The complete disorder model (excluding H atoms) consists of component 1, [P(1), C(331), C(341), C(351), C(361), C(371) C(381)], component 2 [P(11), C(33), C(34), C(35), C(36), C(37), C(38)] , and component 3 [P(12), C(332), C(342), C(352), C(362), C(372), C(382), C(271, C(281), C(291), C(301), C(311), C(321)]. All atoms with occupancies < 0.9 were refined using isotropic displacement parameters. Final least-squares refinement converged to $R_1 = 0.0420$ ($I > 2\sigma(I)$, 8321 data) and $wR_2 = 0.1228$ (F^2, 10137 data, 508 parameters). The final CIF is available as supporting material.

Figure S23: DFT optimized structures of compounds **A**: (PPP)NiCl (**8**), **B**: [(PPP)Ni]^0 (**10'**), **C**: [(PPP)Ni]$^+$ (**12'**), and **D**: [(PPP)Ni]$_2^+$ (**13**)

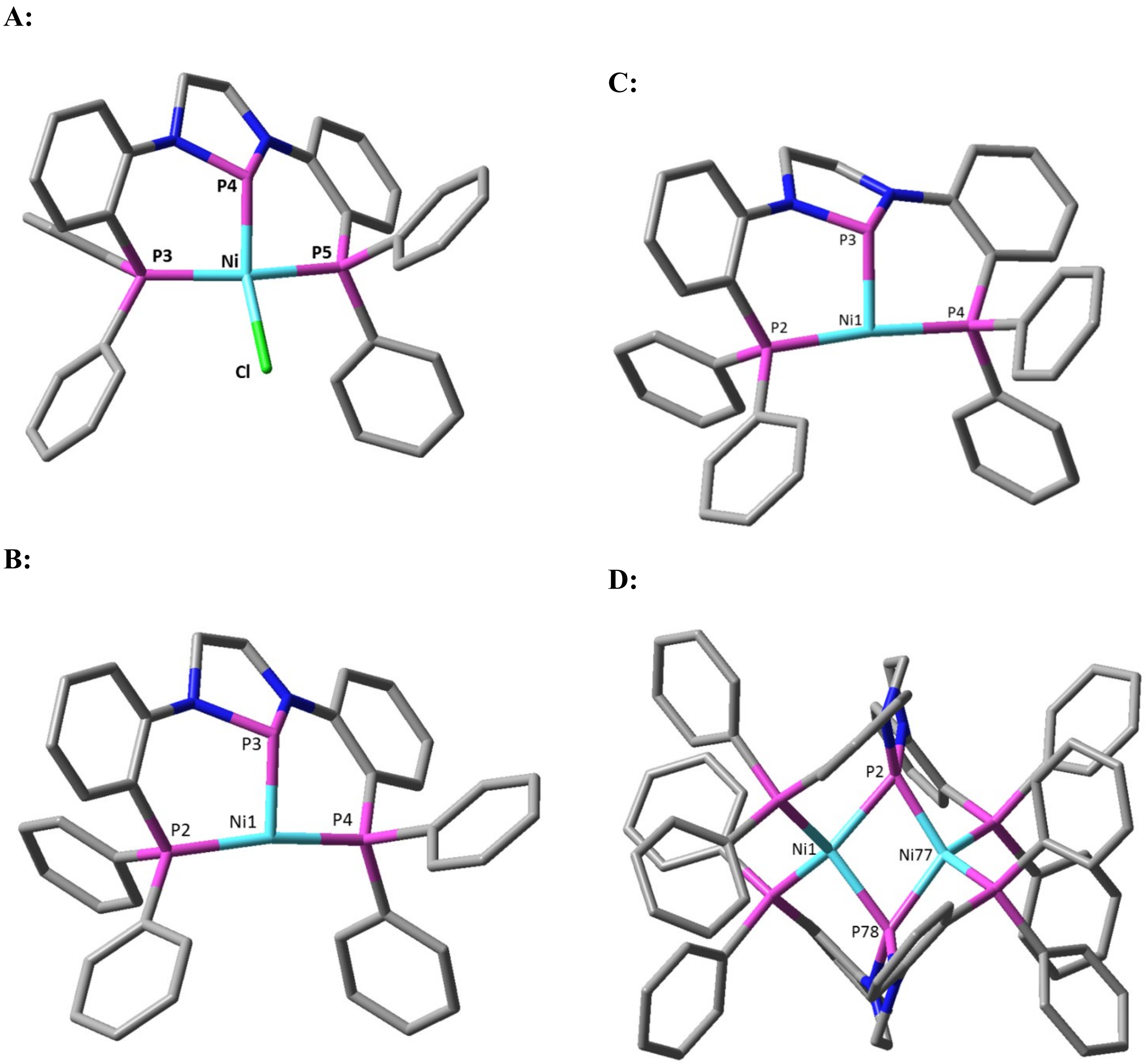

Table S2: Comparison of selected experimental and calculated bond lengths for (PPP)NiCl (**8**)

Bond/Angle	Experimental (X-ray)	Calculated (DFT)
P2^{central}-Ni	2.0903(7) Å	2.12 Å
P1^{side}-Ni	2.2092(6) Å	2.23 Å
P3^{side}-Ni	2.1705(6) Å	2.24 Å
Cl-Ni	2.2402(7) Å	2.25 Å
∠P2NiP1	83.499(24)°	90.4°
∠NPN	89.940(94)°	88.9°
∠P2NiP3	88.897(24)°	84.9°
∠P1NiP3	149.479(23)°	156.9°
∠P2NiCl	143.881(28)°	152.3°
∠P1NiCl	96.647(25)°	100.9°
∠P3NiCl	106.576(25)°	93.4°

Table S3: Calculated bond lengths and angles of [(PPP)Ni]^0 **10’**

Bond/Angle	Calculated
P2^{side}-Ni1	2.19 Å
P3^{central}-Ni1	2.14 Å
P4^{side}-Ni1	2.19 Å
∠NPN	88.6°
∠P3NiP2	97.9°
∠P3NiP4	92.4°
∠P4NiP2	163.4°

Table S4: Calculated bond lengths and angles of [(PPP)Ni]$^+$ **12’**

Bond/Angle	Calculated
P2^{side}-Ni1	2.21 Å
P3^{central}-Ni1	2.11 Å
P4^{side}-Ni1	2.22 Å
∠NPN	91.3°
∠P3NiP2	96.8°
∠P3NiP4	89.6°
∠P4NiP2	173.1°

Table S5: Calculated bond lengths and angles of $[(PPP)Ni]_2^+$ **13**

Bond/Angle	**Calculated**
P2^{central}-Ni1	2.26 Å
P2^{central}-Ni77	2.12 Å
P78^{central}-Ni1	2.26 Å
P78^{central}-Ni77	2.12 Å
P6^{side}-Ni1	2.32 Å
P119^{side}-Ni1	2.32 Å
P43 ^{side}-Ni77	2.25 Å
P82 ^{side}-Ni77	2.25 Å
Ni1-Ni77	2.59 Å
∠P2-Ni1-P6	88.1°
∠P2-Ni1-P119	134.5°
∠P2-Ni1-P78	102.5°
∠P6-Ni1-P119	115.6°
∠P6-Ni1-P78	134.5°
∠P119-Ni1-P78	88.1°
∠P2-Ni77-P43	90.3°
∠P2-Ni77-P82	123.4°
∠P2-Ni77-P78	112.3°
∠P43-Ni77-P82	120.1°
∠P43-Ni77-P78	123.4°
∠P82-Ni77-P78	90.3°

A text file of all the computed molecule Cartesian coordinates in .xyz format for convenient visualization is available as supporting material.

Figure S24: DFT calculated NBOs: Ni-P NBOs observed in [(PPP)Ni]$^+$ (**12’**)

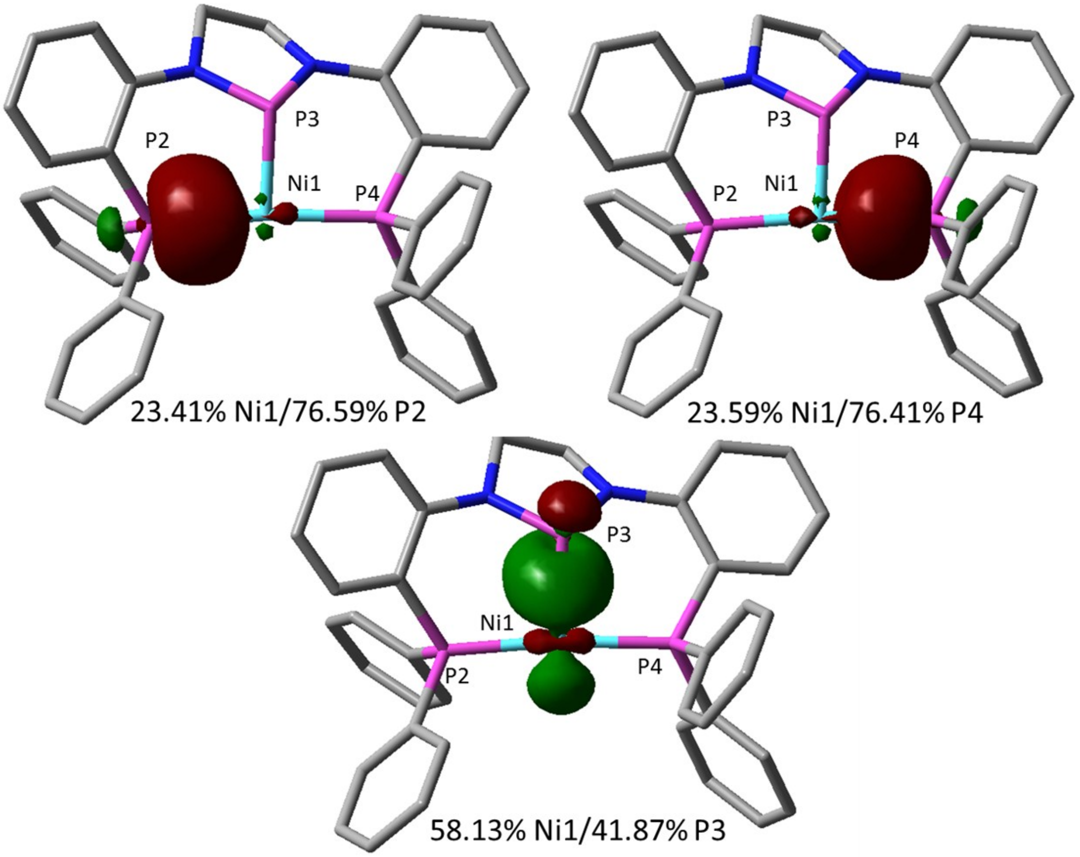

23.41% Ni1/76.59% P2

23.59% Ni1/76.41% P4

58.13% Ni1/41.87% P3

Figure S25: DFT calculated NBO: Lone pair on NHP phosphorus atom of **12’**

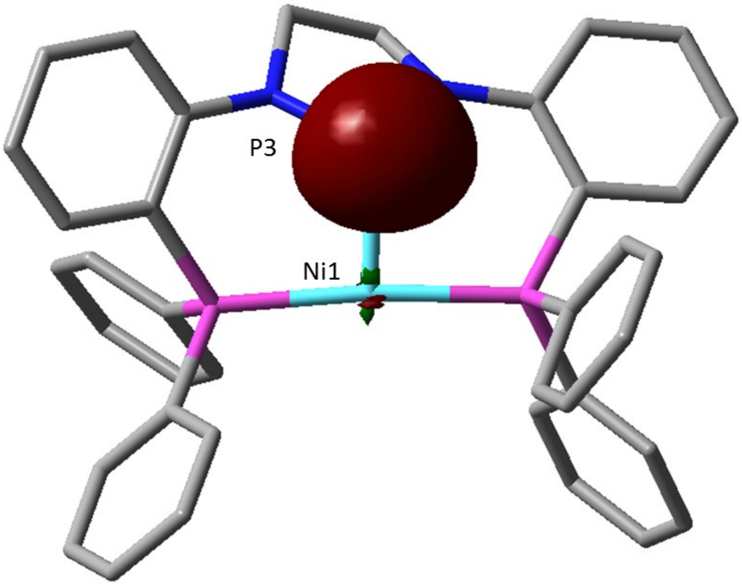

Figure S26: UV-vis NIR spectra for [(PPPNi)]$_2$ **10** (THF), [(PPPNi)]$_2$[PF$_6$]$_2$ **12** (DCM) and [(PPPNi)]$_2$[PF$_6$] **13** (DCM)

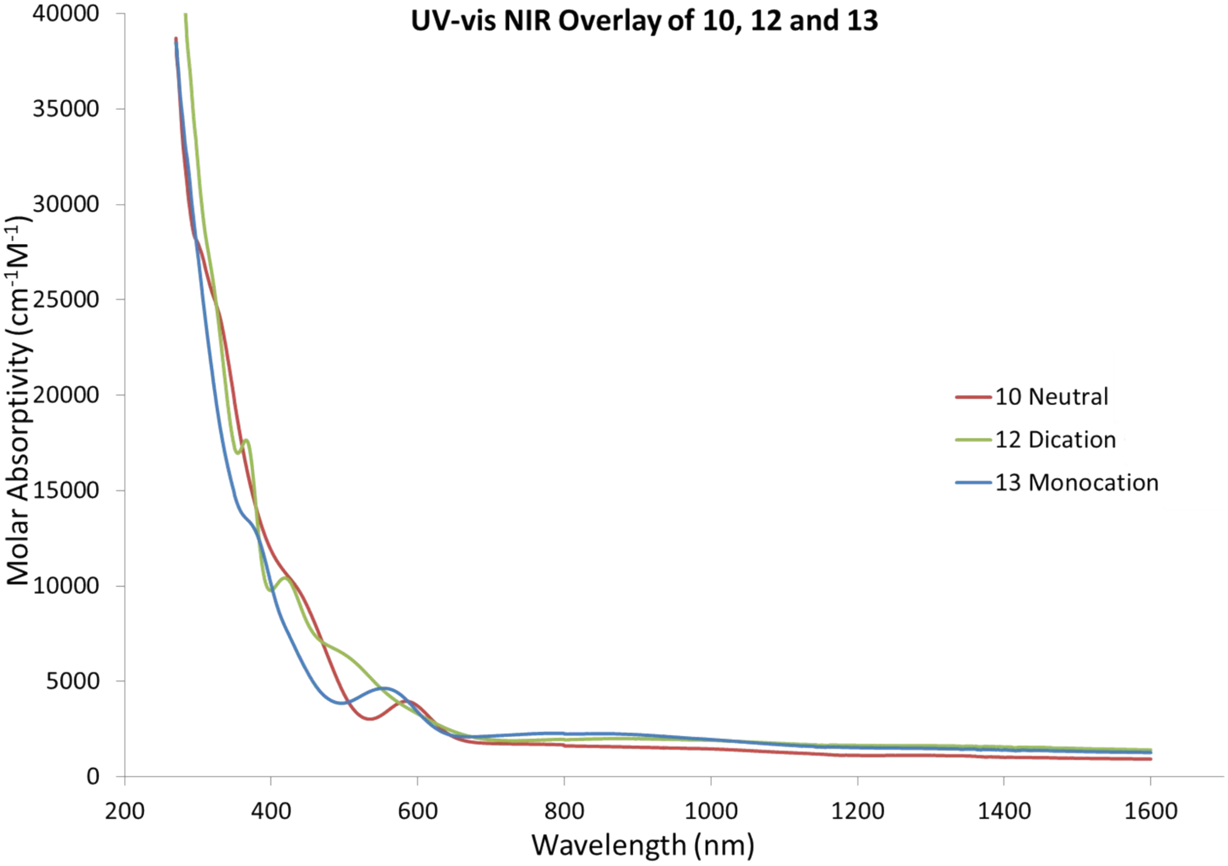

Full Gaussian09 Reference:
M. J. Frisch, G. W. Trucks, H. B. Schlegel, G. E. Scuseria, M. A. Robb, J. R. Cheeseman, G. Scalmani, V. Barone, B. Mennucci, G. A. Petersson, H. Nakatsuji, M. Caricato, X. Li, H. P. Hratchian, A. F. Izmaylov, J. Bloino, G. Zheng, J. L. Sonnenberg, M. Hada, M. Ehara, K. Toyota, R. Fukuda, J. Hasegawa, M. Ishida, T. Nakajima, Y. Honda, O. Kitao, H. Nakai, T. Vreven, J. A. Montgomery, Jr., J. E. Peralta, F. Ogliaro, M. Bearpark, J. J. Heyd, E. Brothers, K. N. Kudin, V. N. Staroverov, R. Kobayashi, J. Normand, K. Raghavachari, A. Rendell, J. C. Burant, S. S. Iyengar, J. Tomasi, M. Cossi, N. Rega, J. M. Millam, M. Klene, J. E. Knox, J. B. Cross, V. Bakken, C. Adamo, J. Jaramillo, R. Gomperts, R. E. Stratmann, O. Yazyev, A. J. Austin, R. Cammi, C. Pomelli, J. W. Ochterski, R. L. Martin, K. Morokuma, V. G. Zakrzewski, G. A. Voth, P. Salvador, J. J. Dannenberg, S. Dapprich, A. D. Daniels, O. Farkas, J. B. Foresman, J. V. Ortiz, J. Cioslowski, and D. J. Fox, Gaussian, Inc., Wallingford CT, 2009.

References

1. *Apex 2, Version 2 User Manual, M86-E01078*. 2006.
2. Altomare, A. C., G.; Giacovazzo, G.; Guagliardi, A.; Burla M. C.; Polidori, G.; Camalli M. , *J. Appl. Cryst.* **1994,** *27*.
3. Betteridge, P. W. C., J. R.; Cooper, R. I.; Prout, K.; Watkin, D. J. , *J. Appl. Cryst.* **2003,** *36*.
4. Cooper, R. I. T., A. L.; Watkin, D. J. , *J. Appl. Cryst.* **2010,** *43*, 1100-1107.
5. Macrae, C. F. B., I. J.; Chisholm, J. A.; Edgington, P. R.; McCabe, P.; Pidcock, E.; Rodriguez-Monge, L.; Taylor, R.; van de Streek, J.; Wood, P. A. , *J. Appl. Cryst.* **2008,** *41*, 466-470.
6. (a) Spek, A. L., *Acta Crystallogr., Sect A* **1990,** *A46*, C34; (b) Spek, A. L., *PLATON, A Multipurpose Crystallographic Tool* Utrecht University: Utrecht, The Netherlands, 1998.
7. v. d. Sluis, P. S., A., *Acta Crystallogr., Sect. A* **1990,** *A46*, 194-201.
8. Palatinus, L. C., G. , *J. Appl. Cryst.* **2007,** *40*, 786.